

Peer review status:

This is a non-peer-reviewed preprint submitted to EarthArXiv.

1 **Hydraulic Fracturing in a Confined Space System: Stress State, Fracture Space, and**

2 **Production Enhancement Mechanism**

3 Yang Yang

4 Weiyang District, Xi'an 710021, Shaanxi, China

5 Corresponding author. E-mail address: geospetro@gmail.com (Y. Yang)

6

7 **Abstract:** Existing mechanical models for hydraulic fracturing technology are established based on open
8 space systems, assuming fractures are primarily formed through tensile failure. However, the source
9 mechanism of newly created fracture space under confined space conditions with constant total volume
10 remains unclear. This study develops a mechanical model for hydraulic fracturing in confined space
11 systems based on fundamental principles including volume conservation, pore volume redistribution,
12 Newton's third law, and Pascal's law. The research demonstrates that: the formation of artificial fractures
13 and accommodation space for proppants originates from the adjustment and redistribution of existing pore
14 space; compressive differential deformation provides the mechanical basis for shear fracture formation;
15 rock deformation and failure follow an evolutionary sequence of "compression (generating fracture space)
16 → tension (controlling fracture propagation direction) → differential deformation (forming shear
17 fractures)."Based on the newly established mechanical model and Biot's poroelastic coupling theory, a
18 novel fracturing production enhancement mechanism is proposed. This mechanism can provide theoretical
19 guidance for well placement, wellbore trajectory design, and hydraulic fracturing target optimization,
20 contributing to improved reservoir utilization and recovery rates, while offering new theoretical
21 foundations for reservoir development numerical simulation..

22 **Highlights**

23

24 (1)The artificial fractures and proppant-accommodating spaces formed in a confined space
25 system are the result of the adjustment and redistribution of the existing pore space.

26 (2)The increase in reservoir fluid pressure and fracture space are the controlling factors of
27 fracturing production increase.

28 (3)The compaction of the formation after reservoir formation, the secondary enlargement of
29 diagenetic minerals, and the expansion of clay minerals can all increase the pressure of the
30 reservoir fluid.

31 (4)The three-dimensional distribution of porosity and the reservoir fluid pressure parameters

32 after fracturing can be used to quantitatively evaluate the effect of hydraulic fracturing and
33 predict production.

34

35 **Keywords:** Confined space system; Pore volume redistribution; Fracture space; Biot's
36 poroelastic coupling theory; Oil enhancement mechanism

37

38 **1. Introduction**

39 Hydraulic fracturing has long been regarded as a key stimulation technique for
40 enhancing the recovery of low-permeability oil and gas reservoirs. Since the 1950s, when
41 Hubbert and Willis proposed the classical linear elastic fracture model (Hubbert and Willis,
42 1957)[8], it has been assumed that fractures form in an infinite or semi-infinite homogeneous
43 elastic medium in a tensile mode. Subsequently, the PKN and KGD[1][11] models were
44 developed by Perkins and Kern (1961) [13]and Geertsma and de Klerk (1969), respectively,
45 to describe the planar propagation characteristics of fractures (Perkins and Kern, 1961;
46 Geertsma and de Klerk, 1969)[4][5][6]. In recent years, models such as the Finite Element
47 Method (FEM), Discrete Fracture Network (DFN) (Berkowitz, 2002, Olson, J.E., &
48 Dahi-Taleghani, A. 2010) [2,12], and phase-field fracture models(Miehe et al., 2010)[7] have
49 significantly advanced our understanding of fracture propagation, stress redistribution, and
50 fracture conductivity. However, these conventional models commonly assume that fracture
51 propagation occurs in an open or semi-infinite elastic medium, neglecting the spatial
52 confinement of real geological formations. Moreover, they diverge significantly from the
53 complex fracture networks (including shear fractures) observed in modern volume fracturing
54 through microseismic monitoring(Fisher, M.K., & Warpinski, N.R. 2012 , Warpinski et
55 al.,Warpinski et al., 2009)[5][16]. This fundamental assumption is now facing serious
56 challenges in the context of widespread application of modern volume fracturing
57 technologies.

58 With the rise of shale gas and tight oil development, massive volume fracturing
59 technology has been widely applied. Unlike traditional small-scale fracturing, volume
60 fracturing involves massive injection volumes—typically millions of pounds of proppant and
61 tens of thousands of cubic meters of fracturing fluid. This high-intensity, large-volume
62 operation creates a complex multi-stage fracture network around the wellbore, significantly
63 enhancing the reservoir's flow capacity (Economides and Nolte, 2000)[4] and enabling
64 overall optimization of reservoir stimulation (Mayerhofer et al., 2010)[9].However, this
65 large-scale injection of fluids and solids raises a fundamental and critical question: where

66 does the internal space within the formation come from to accommodate such a vast volume
67 of injected materials? Traditional theories have primarily focused on fracture opening and
68 conductivity, assuming that as long as failure criteria are met, sufficient fracture space will
69 naturally be generated. Yet, they largely overlook the fundamental physical issue of spatial
70 availability. Prior to the work presented in this paper, there has been virtually no systematic
71 research addressing this “volume constraint” problem—how exactly the formation
72 accommodates these injected materials within a confined underground space remains an
73 underappreciated and insufficiently understood issue.

74 To address this fundamental issue, this study proposes a new mechanical model for
75 hydraulic fracturing under confined space constraints. Within this framework, fracture
76 formation is no longer viewed as a purely tensile failure process, but rather as a volume
77 reconfiguration process driven by compressive deformation, pore collapse, and localized
78 shear failure. This model introduces the fundamental principles of rock volume conservation
79 and pore space redistribution, and draws upon Biot’s theory of poroelasticity in porous
80 media (Biot, 1941)[3]. It emphasizes that the creation of any new fracture space must be
81 accompanied by a reduction in existing pore volume. This perspective breaks away from the
82 traditional assumption that “fracture propagation equals space creation,” and also rejects the
83 notion of “volume expansion” as a valid explanation. Instead, it redefines the mechanical
84 essence of fracture formation under realistic geological constraints.

85 Building upon this new model, the paper further reveals an enabling mechanism for
86 production enhancement through hydraulic fracturing: the process not only improves flow
87 conditions by creating high-conductivity fractures, but more importantly, the compressive
88 deformation during fracturing significantly reduces the original pore volume, resulting in an
89 increase in the internal fluid pressure of the reservoir. This elevated pressure not only
90 enhances the mechanical driving force for hydrocarbon migration toward the wellbore but
91 also partially overcomes the confining effect of surrounding rock, thereby mobilizing more
92 reservoir fluids and potentially converting isolated pores into interconnected ones. Therefore,
93 the essence of production enhancement lies not only in creating new flow pathways, but also
94 in mechanically empowering and pressure-activating the reservoir system. This novel
95 perspective not only broadens the scope of conventional fracturing theory but also provides
96 new insights for fracturing design and production forecasting.

97 In addition, this new model holds significant practical value in reservoir stimulation,
98 production enhancement design, and economic evaluation. By introducing the concept of
99 pore space redistribution, it enables more accurate prediction of effective proppant

100 placement efficiency, thereby optimizing fracture space design and improving proppant
101 utilization. Moreover, based on the newly proposed mechanism of reservoir pressure
102 elevation, the model facilitates more effective selection of injection pressure and fluid
103 volume, enhancing the efficiency of fracturing fluid usage and reducing operational costs.
104 Furthermore, the model allows for more precise assessment of stimulation effectiveness,
105 offering theoretical support for the optimization of reservoir development strategies. Overall,
106 it demonstrates strong potential for impactful engineering applications in unconventional
107 reservoir development.

108 The remainder of this paper is organized as follows: Section 2 presents the theoretical
109 foundation of the confined-space mechanical model in detail, including stress analysis,
110 boundary conditions, volume balance equations, and fracture criteria. Section 3 validates the
111 proposed model based on the characteristics of microseismic activity. Section 4 discusses the
112 origin of fracture space, the production enhancement mechanism, fracture conductivity, and
113 new perspectives for numerical simulation. Section 5 elaborates on the new mechanism of
114 production enhancement and its implications for fracturing design and reservoir development
115 strategies.

116

117 **2. Stress Field in a Confined Space System**

118 **2.1 Key Conceptual Definitions**

119 **2.1.1 Confined Space System**

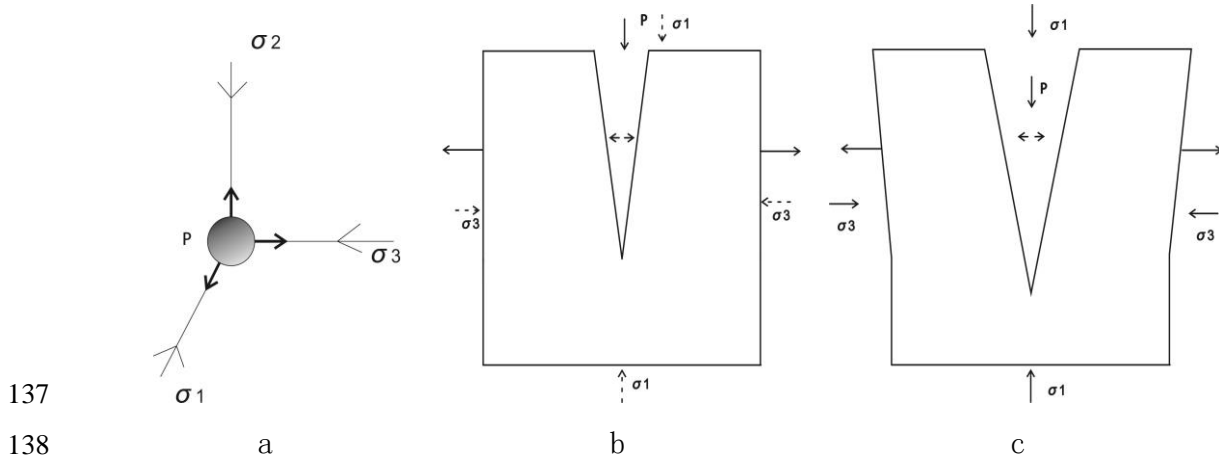
120 A confined space system refers to a relatively closed domain filled with both fluid and
121 rock, within which the rock cannot move freely. According to Newton's Third Law, the
122 presence of high-pressure fluid in such a system necessarily implies a reactive force exerted
123 by the surrounding rock, thus forming a pair of action and reaction forces.

124 When large-scale hydraulic fracturing is considered within a confined space system,
125 both total volume (rock volume + pore volume before fracturing) and pore volume are
126 subject to conservation principles. The space required for the formation of new fractures
127 during fracturing is obtained through the adjustment and redistribution of pre-existing pore
128 space, which simultaneously serves as the accommodation space for a large amount of
129 proppant. While the total volume remains constant, its composition changes to: rock volume
130 + pore volume (after fracturing) + proppant volume.

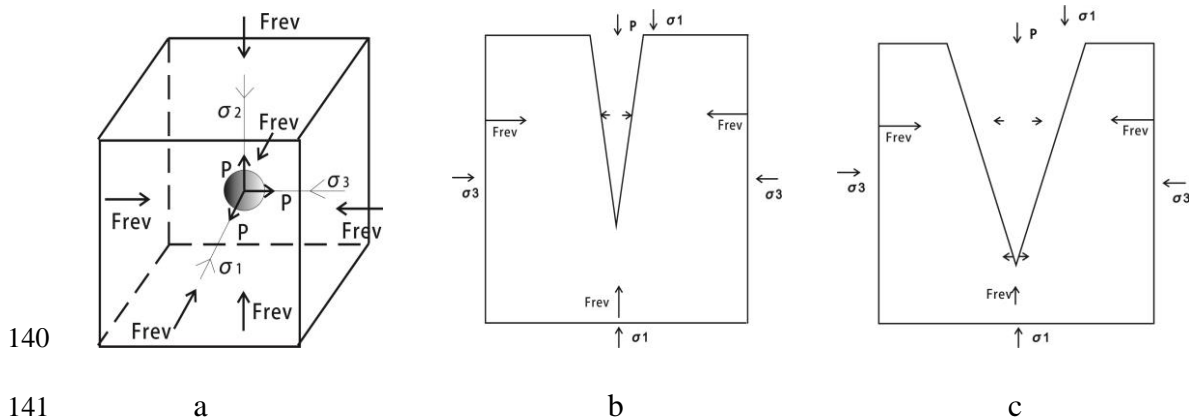
131 **2.1.2 Stress State**

132 In conventional models, which assume an open-space system (with unlimited and freely
133 expandable volume), tensile stress is not opposed by any reactive force, resulting in a

134 non-compressive environment that allows free tensile opening. The stress condition can be
 135 expressed as: fluid pressure > minimum principal stress + tensile strength → fracture
 136 opening (tension-dominated).



137
 138
 139 **Fig. 1** Stress state and 2D fracture propagation model under an open-space system



140
 141
 142 **Fig. 2** Stress state and 2D fracture propagation model under a confined-space system

143 In the new model, the system is a confined space system, where the target formation is
 144 surrounded by a relatively closed boundary and no free tensile expansion space exists. The
 145 high-pressure fluid and its reactive force together create a compressive environment. The
 146 stress condition follows the sequence: fluid pressure → compressive stress on rock →
 147 adjustment and redistribution of existing pore space into fracture space (compression- and
 148 shear-dominated) → crack tip opening (tension-dominated) → control of fracture
 149 propagation direction.

150 The core of this transition lies in changing the system from an open space to a confined
 151 space, where fluid pressure shifts from being the main driver for tensile fracturing to the
 152 driving force for compressing the rock. Consequently, the stress state changes from free
 153 tensile deformation to compression.

154 **2.2 Mechanical Model**

155 **2.2.1 Force Analysis, Boundary Conditions, and Stress State under Confined Space**

156 **Boundary Conditions:** Triaxially confined (rock formation boundaries exist in X, Y, and Z
157 directions), with no free volumetric expansion allowed.

158 **Loading Mode:** Pressure is transmitted to pores and weak planes through fluid conduction;
159 loading is slow and continuous, with gradual pressure variation.

160 **Stress State:** A coupled stress field dominated by compressive and shear stresses is formed,
161 supplemented by tensile failure at fracture tips and pore volume compression.

162 **Fracture Criterion:** Based on the Mohr-Coulomb failure criterion.

163 **Fracture Path:** Governed mainly by differential stress, distribution of structural weak planes,
164 and pore space redistribution; macroscopically, fracture propagation remains constrained by
165 the minimum principal stress direction.

166 **Fracture Width Origin:** Formed by compaction-driven reconfiguration rather than simple
167 tensile “opening.”

168 **Constraints:** Conservation of total volume, conservation of pore space volume, Newton’s
169 third law, and Pascal’s law.

170 **2.2.2 Rock Stress State under Confined Space**

171 **2. 2. 2. 1 Definition of Key Variables**

172 P: External high-pressure fluid pressure

173 σ_3 : Minimum principal stress

174 σ_1 : Maximum principal stress

175 S_c : Compressive strength

176 S_s : Shear strength

177 S_t : Tensile strength

178 ϕ : Rock porosity (affects strength parameters)

179 F_{rc} : Reactive force in compression direction

180 F_{rs} : Reactive force in shear direction

181 F_{rt} : Reactive force in tensile direction

182 V_{pre} : Pore volume before fracturing

183 V_{pro} : Pore volume after fracturing

184 V_{fra} : Volume of new fracture space

185 V_{pr} : Proppant volume

186 **2. 2. 2. 2 Stress State and Analysis under Confined Space Constraints**

187 **Force analysis in minimum principal stress direction:**

188 Resultant force $\sigma = P - \sigma_3$ (1)

189 Force analysis in maximum principal stress direction:

190 Resultant force $\sigma = \sigma_1 - P$ (2)

191 Compression direction:

192 Reactive force equals external high-pressure fluid pressure

193 $F_{rc} = P$ (3)

194 Location of shear failure:

195 The magnitude of the reaction force is determined by the magnitude of the external
196 high-pressure fluid.

197 Location of tensile failure:

198 The magnitude of the reaction force is determined by the magnitude of the external
199 high-pressure fluid.

200 Volume conservation:

201 Total volume before fracturing equals rock matrix plus pore volume

202 $V_{pre} = V_{rock} + V_{pre}$ (4)

203 Total volume after fracturing equals matrix volume plus post-fracture pore volume plus
204 proppant volume:

205 $V_{pro} = V_{rock} + V_{pro} + V_{pr}$ (5)

206 Pore volume conservation:

207 Post-fracture pore volume equals pre-fracture pore volume minus new fracture volume

208 $V_{pro} = V_{pre} - V_{fra}$ (6)

209 Proppant volume approximately equals new fracture space volume:

210 $V_{pr} \approx V_{fra}$ (7)

211 For porous rocks, the compressive strength, shear strength, and tensile strength are all
212 closely related to porosity, and this relationship must be taken into account in the model.

213 In a confined space system, the total pore volume remains conserved (note that after
214 fracturing, part of the pore space is occupied by proppant, and this must be considered when
215 establishing the equations). The amount of solid material increases (due to the addition of
216 proppant), while fluid can flow unidirectionally—typically, high-pressure fluid enters the
217 formation, generating local high-pressure zones that displace the original formation fluids
218 toward lower-pressure regions.

219 **2.2.3 Fracture Initiation Conditions**

220 In an open-space system, fracture initiation does not require overcoming reactive forces.

221 However, in a confined space system, the rock can only fracture after overcoming the

222 reactive forces and disrupting the existing mechanical equilibrium.

223 To determine whether rock failure occurs, the following criteria can be used:

224 ① Compressive Fracture: $P > F_{rc}$ (8)

225 ② Tensile Fracture: $P_f > F_{rt}$

226 ③ Shear Fracture:

227 In confined systems, the reactive force F_{rs} must be incorporated as a
228 correction term: $\tau > (\sigma_n + F_{rs}) \tan \phi$ (9)

229 **2.3 Feasibility Analysis of the New Model**

230 **2.3.1 Mechanical Implications of Different Spatial Types**

231 In an open-space system, a unidirectional force source can independently produce
232 deformation effects. The pressure exerted by high-pressure fluid on the formation rock is not
233 constrained by any opposing force from the surrounding rock, allowing the rock to move
234 freely (see Fig. 1c).

235 In a confined-space system, however, the rock cannot move freely. The externally
236 applied pressure is met with a reactive force from the surrounding formation, together
237 forming a compressive interaction (see Fig. 2b).

238 Conventional perspective: Fluid pressure P_{pp} applies stress directly on the fracture
239 walls (see Figs. 1b and 1c), but lacks a counteracting force, allowing free tensile opening.

240 New perspective: In a confined-space system, the presence of boundary constraints
241 means that fluid pressure P_{pp} , together with its reactive force, applies compressive stress on
242 the rock and fracture surfaces, manifesting as a compression-dominated process (see Figs. 2b
243 and 2c).

244 **2.3.2 Changes in Pore Volume Within Rock**

245 The space generated when rock is subjected to compression consists of two components:
246 (1) elastic deformation of the rock matrix, and (2) redistribution of space from the
247 compression of pre-existing pores.

248 Under subsurface compressive stress conditions, the rock is already in a state of elastic
249 deformation. Any additional pressure beyond this state will exceed the elastic limit and result
250 in rock failure. Therefore, it is unnecessary to attribute the creation of
251 proppant-accommodating space to elastic volume reduction. Instead, both the fracture space
252 and the space for proppant placement originate from the adjustment and redistribution of
253 pre-existing pore space

254 **2.3.3 Formation of Fracture Space under Compression**

255 Under a compressive stress environment, fracture formation is no longer a pure opening

256 mode (Mode I), but rather involves compression-induced localized deformation. Rocks
257 between regions of high-pressure fluid are under strong compression, causing collapse of
258 various pore types within the rock. The space released from this collapse, after redistribution,
259 becomes the space available for proppant placement. Differential compressive deformation
260 can also induce shear slip (Mode II or III), leading to the formation of secondary fractures
261 intersecting with the main fracture, characterized as shear fractures (see Fig. 3b).

262 **2.3.4 Increase in Reservoir Pressure after Fracturing**

263 In a reservoir system, pore space exists prior to the establishment of fluid pressure
264 within those pores. The pressure in the pores is determined by the degree of fluid filling, not
265 by burial depth. For an isolated pore, the internal pressure is independent of depth and is
266 solely a function of its fluid saturation. Therefore, reduction of pore volume is the key factor
267 leading to an increase in reservoir pressure, a concept that aligns with Biot's poroelastic
268 theory of fluid-solid coupling in porous media.

269

270 **3. Validation of the New Theory by Microseismic Observations**

271 Conventional theory holds that the dominant fractures generated during hydraulic
272 fracturing are of tensile nature. However, monitoring results from massive volume hydraulic
273 fracturing operations have revealed a significant number of shear fractures, which are often
274 interpreted as the result of shear slip along pre-existing faults or fractures. Even if such shear
275 slip occurs, it presupposes the existence of available space for displacement—yet
276 conventional models do not explain where this physical space comes from during the slip
277 process.

278 The new mechanical model under the confined-space system proposes that differential
279 compressive deformation of the rock is the key factor responsible for shear fracture
280 formation. Vavrycuk et al. (2008)[14] noted that the non-double-couple components
281 observed in seismic moment tensors during fluid injection at the German KTB super-deep
282 borehole were most likely caused by rock anisotropy, rather than tensile opening. Vavrycuk.
283 Their conclusion was based on the presence of negative CLVD components, which are
284 inconsistent with tensile fracturing. Furthermore, these seismic events were triggered at fluid
285 pressures far below the fracturing gradient (Zoback and Harjes, 1997)[18][19], making
286 tensile failure unlikely. Notably, this phenomenon is also observed in microseismic events
287 associated with hydraulic fracturing in unconventional reservoirs. These events occur in
288 highly anisotropic formations, and are triggered by fluid pressures well below the fracture
289 gradient. From this, it can be concluded that: under the same fluid pressure, rock anisotropy

290 can result in differential compressive deformation, supporting the core mechanism proposed
291 in the new model.

292

293 **3.1 Validation from Microseismic Spatial Distribution**

294 Zhang et al. (2018) [17] reported the presence of dense clusters of microseismic events
295 during multi-stage fracturing operations, with event magnitudes decreasing from the center
296 outward. While this phenomenon was previously attributed to fracture complexity, our model
297 suggests it is a natural result of compressive stress redistribution under confined-space
298 constraints. Zhang.

299 As the compressive stress front propagates outward, the availability of pore space
300 decreases, and the rock becomes increasingly compacted, leading to smaller-magnitude
301 microseismic events in the peripheral areas.

302 Energy dissipation becomes more dispersed and lower in intensity, which corresponds to
303 the observed decrease in seismic magnitude.

304 Thus, the attenuation of magnitudes from center to edge is not merely a function of
305 fracture complexity, but a predictable outcome of stress redistribution under confined spatial
306 conditions.

307 This pattern reflects both the consumption of compressible pore space and the
308 diminishing capacity of the system to accommodate slip or fracture growth as it seeks a new
309 equilibrium under pressure.

310 **3.2 Validation of Shear-Dominated Microseismic Mechanisms**

311 In the study by Wang et al. (2021)[15], over 70% of microseismic events exhibited
312 shear-dominated mechanisms. This aligns with our theoretical prediction: under constrained
313 conditions, shear fractures are generated due to differential compressive deformation.

314 In hydraulic fracturing, the target formation is surrounded by rock layers that
315 mechanically constrain deformation of the pressurized volume. These confined-space
316 conditions prevent free expansion in all directions, especially in horizontal planes where
317 adjacent rock masses remain stationary. Therefore, any volume increase due to fluid
318 injection must be accommodated via internal reconfiguration.

319 As fluid enters the formation, pressure radially displaces rock material. However, lateral
320 displacement is restricted by spatial boundaries, leading to the accumulation of horizontal
321 compressive stress. Unless critical thresholds are reached, these stresses are insufficient to
322 initiate new tensile fractures—but they do promote shear failure along pre-existing or
323 stress-induced weak planes.

324 Mechanism Preference under Constraints: Under such stress conditions, Coulomb
325 failure (which governs shear activation) is more likely to occur than tensile failure (which
326 controls Mode I opening). Shear fractures require less net displacement and are more
327 compatible with spatial confinement, giving them a mechanical advantage. Therefore, the
328 high proportion of shear-dominated events is a natural outcome of the system seeking
329 low-energy deformation pathways within a restricted environment.

330 Implications for Fracture Interpretation: The observed dominance of shear mechanisms
331 reflects the primary stress paths in laterally constrained compressive environments. It also
332 indicates that fracture propagation is not solely pressure-driven, but is strongly controlled by
333 the degrees of freedom available in the surrounding medium.

334 **3.3 Evolutionary Trends in Microseismic Magnitude**

335 The microseismic clustering and magnitude attenuation observed by Maghsoudi et al.
336 (2016)[8] can be reinterpreted within the framework of the confined-space stress model. In
337 this framework, spatially limited pore spaces are progressively compressed under
338 injection-induced stress. Initially, large amounts of energy are released through shear or
339 compressive failure. As the available compressible space is gradually exhausted, the system
340 transitions into a redistribution phase, during which microseismic activity continues, but
341 with decreasing event magnitudes and increasing spatial dispersion.

342 In a closed or confined system, energy release must occur through progressive
343 compression and shear-slipping transitions. The power-law characteristics of the observed
344 magnitude distribution reflect the system's inability to sustain continued fracture extension
345 due to spatial constraints. Instead, energy is released through localized slip and shear
346 deformation, with the energy released per event diminishing over time, forming a power-law
347 distribution of event scales.

348 During the initial stage of fracturing, injected fluids rapidly enter natural pores or
349 pre-existing weak planes, which are relatively easy to compress. In a confined space, the
350 compressive stress field induced by fluid injection becomes concentrated in these localized
351 regions. As a result, microseismic events are clustered within these
352 "compression-shear-prone zones," forming what is known as non-uniform clustering.

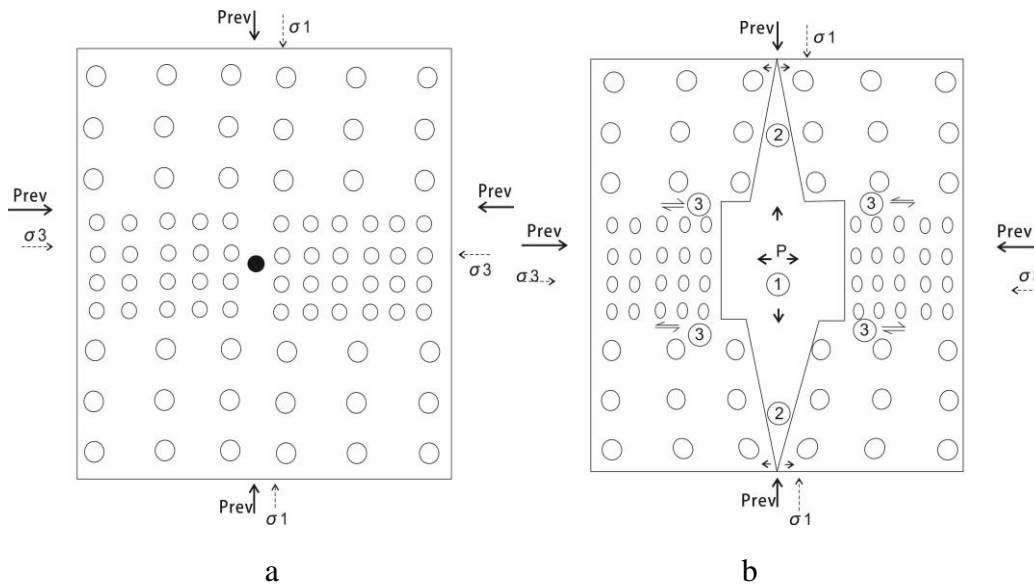
353

354 **4. Discussion**

355 **4.1 The Stress Field Responsible for New Fracture Formation Is Compressional in Nature**

356 Traditional theories are based on mechanical models developed under open-space
357 system assumptions, which implicitly presume that the formation is an open

358 system—unconstrained by the surrounding rock and able to provide unlimited space for
 359 fracture propagation. Under the action of high-pressure fluid, it is assumed that the minimum
 360 principal stress is reversed from compression to tension, thereby inducing fracture
 361 opening—i.e., a tensile-dominated stress regime.



362
 363

364 **Fig. 3** Pore compression and rock failure stages in a confined-space system

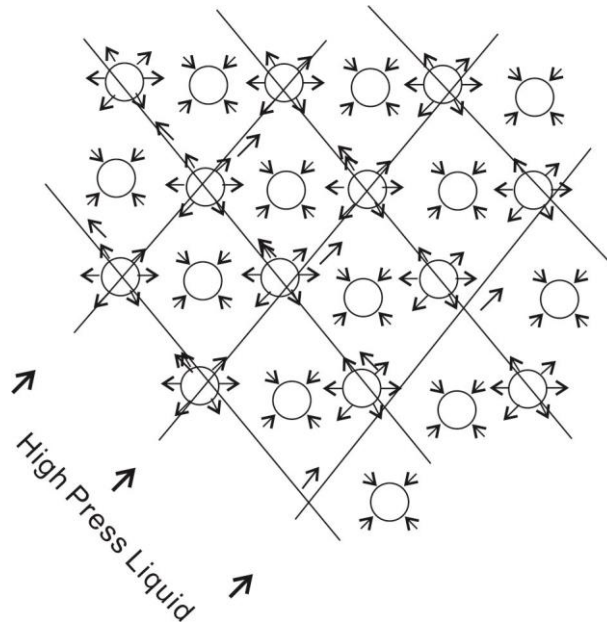
365 In reality, the subsurface within a confined domain is completely filled with rock, and
 366 any fracture propagation requires additional space. The surrounding rocks within this finite
 367 domain are subject to confinement forces from adjacent formations.

368 In such a confined environment, even if the high-pressure fluid alters the direction of the
 369 minimum principal stress, Newton’s Third Law dictates that the reactive force (resulting
 370 from both compressive and shear strength) counters the fluid pressure, forming a
 371 force-reaction pair. This means the formation of new fractures is driven by compression of
 372 the existing pore space by the high-pressure fluid, thereby creating space for new fractures.
 373 In other words, it is compressive and shear actions that generate new fractures—indicating
 374 that the stress field is fundamentally compressional.

375 The fracture width is a result of this compressive action. It not only provides space for
 376 proppant placement but also serves as a critical flow conduit for hydrocarbons within the
 377 reservoir. Furthermore, it is a key factor contributing to increased reservoir pore pressure and
 378 enhanced hydrocarbon production.

379 Fracture extension, on the other hand, is the result of tensile action caused by bulk rock
 380 displacement. As more high-pressure fluid is injected into the confined space, the distance
 381 between the walls of the main fracture increases, leading to bulk movement of the rock on

382 both sides of the fracture. The driving force comes from overcoming the shear strength,
383 creating tensile conditions at the fracture tip, allowing the main fracture to propagate in
384 tandem with increasing fracture width.



385
386 Fig. 4 Schematic diagram of the stress state after high-pressure fluid enters the rock along the optimal
387 pathway

388 It is essential to clarify: without new space generated by compression, there is no
389 mechanical basis for tensile action at the fracture tip.

390 Shear fractures are the result of differential compressive deformation. When such
391 deformation becomes significant, it induces shear stress conditions between adjacent rock
392 blocks. If the strain is large enough, shear fractures form (see Fig. 3b).

393 Under the traditional open-space model, shear fractures are often attributed to slip along
394 pre-existing natural fractures. However, in reality, subsurface rock is subjected to triaxial
395 compressive stress, and there is insufficient free space to accommodate such slip behavior.

396 Proppant accommodation space arises from adjustment and redistribution of existing
397 pore space. Once high-pressure fluid enters pre-existing spaces (including structural
398 weaknesses), the rock becomes enveloped by the pressurized fluid, including its isolated
399 pores. Under compression, pore volume decreases, and the rock undergoes bulk
400 displacement in the direction opposite to existing voids, thereby forming the fracture
401 width—which also serves as the space for proppant.

402 Thus, under the new mechanical model, the sequential development of fractures is as
403 follows: Compressive deformation creates new space for fracture width; Tensile action
404 occurs at stress-concentrated zones in existing pores, determining the fracture propagation
405 direction; Shear fractures form on both sides of the main fracture due to differential

406 compression (see Fig. 3b).

407 4.2 Reservoir Fluid Pressure Increase as a Key Control Factor in Fracturing-Based 408 Production Enhancement

409 Conventional hydraulic fracturing theories attribute production enhancement primarily
410 to the creation of high-conductivity fractures. In these models, reservoir pressure increase
411 during fracturing is explained by displacement effects. However, this explanation fails to
412 account for the long-term maintenance of elevated reservoir pressure observed after
413 fracturing.

414 In contrast, the new mechanical model under a confined-space system posits that
415 enhanced hydrocarbon productivity after hydraulic fracturing is not primarily due to the
416 creation of new fractures or increased permeability. Rather, it originates from the
417 compression and redistribution of existing pore space (Fig. 3b), which leads to non-uniform
418 increases in pore fluid pressure within the reservoir. A portion of the original
419 hydrocarbon-bearing pore volume is irreversibly transformed into proppant-filled fracture
420 space. This dual mechanism—stress-induced pressure amplification and irreversible pore
421 volume transformation—offers a novel explanation for the sustained productivity observed
422 after large-scale fracturing operations. This insight stems from the application of Biot’s
423 poroelastic theory of coupled fluid-solid behavior in porous media.

424 Under confined-space conditions, massive hydraulic fracturing generates not only new
425 fractures but also leads to reduction of existing pore volumes. As high-pressure fluids follow
426 preferential flow paths into pre-existing pores and flow channels, pressure in these zones
427 rises first. Some fluids are displaced, while pressure in isolated pores increases without
428 displacement. As pore volume gradually decreases, fluid pressure continues to rise. In the
429 case of isolated pores, calculations show that a 1% reduction in pore volume can lead to a
430 pressure increase exceeding 20 MPa (for non-gaseous fluids). When the fluid pressure
431 exceeds the rock’s compressive, shear, or tensile strength, fracture occurs—transforming an
432 isolated pore into a connected flow pathway, thereby improving reservoir connectivity,
433 mobilization, and ultimate recovery (Fig. 4).

434 Displaced fluids move into nearby pores or channels with lower fluid pressure,
435 increasing the local fluid saturation and raising pore pressure. After external high-pressure
436 injection is stopped, the presence of proppant maintains the deformed rock structure and
437 sustains the elevated pore pressure, thereby providing additional driving energy for
438 production. Thus, the role of proppant extends beyond flow conductivity—it also enhances
439 reservoir energy via pressure retention. Therefore, it can be considered that massive

440 fracturing is a coupled process of pore space redistribution and new fracture generation,
441 which results in two key effects: an increase in reservoir fluid pressure and enhanced flow
442 capacity.

443 The post-fracturing reservoir fluid pressure can be used to estimate daily oil production,
444 providing a new foundation for optimizing production strategies.

445 The significance of this perspective lies in:

446 Elevating the concept of “fracture-stimulated productivity” from a geometric
447 interpretation (fracture shape) to one of energy and volume conservation, shifting the focus
448 from “fracture conductivity” to a combined mechanism of fracture conductivity + reservoir
449 energy activation;

450 Providing a more physically consistent explanation for the phenomenon of long-term
451 stable production, reframing the traditional model of “production = increased permeability ×
452 unchanged pressure differential” to “production = flow conduits (fractures) + enhanced
453 driving force (pore compression increasing fluid pressure)”;

454 Establishing a new conceptual bridge between fracturing operations and resulting
455 production behavior;

456 Offering guidance for future fracturing design in low-porosity, pressure-sensitive reservoirs.

457 Misconceptions in the understanding of fracturing mechanisms have led to misaligned
458 objectives in stimulation design. Traditional models view the number of fractures as the sole
459 determinant of productivity, thus making fracture count the primary design target.

460 In contrast, the confined-space model redefines fractures as fluid transport conduits, and
461 emphasizes that compression of existing pores increases fluid pressure, effectively boosting
462 reservoir drive energy—this is the true key to production enhancement. Consequently,
463 expanding the volume of rock subjected to compression should also be a primary objective
464 in fracturing-based stimulation.

465 **4.3 Early Fracture Surface Permeability Determines the Productive Value of Natural** 466 **Fractures**

467 In hydraulic fracturing, not all reactivated natural fractures contribute equally to oil and
468 gas production. A critical but often overlooked factor is the surface flow capacity of the
469 fracture, which refers to the ability of fluids within the rock matrix to migrate across the
470 fracture surface and enter the fracture network. This concept emphasizes the importance of
471 connectivity between the matrix and the fracture surface.

472 Even if a fracture is physically reopened, its contribution to production depends on
473 whether hydrocarbons can effectively flow into the fracture. In many sedimentary formations,

474 natural fracture surfaces or bedding planes are lined with low-permeability minerals, such as
475 calcite films, thin chert layers, or mica sheets. These mineral layers can severely hinder—or
476 even completely block—flow pathways between the porous matrix and the fracture. As a
477 result, even though such fractures may be mechanically open, they remain functionally
478 isolated from the reservoir.

479 This understanding challenges the common assumption that reactivating natural
480 fractures inherently improves production. Instead, it underscores that only fractures with
481 sufficient surface permeability can effectively drain hydrocarbons from the matrix and
482 enhance well performance. Therefore, pre-fracturing treatments targeting mineral barriers on
483 fracture surfaces may improve their surface permeability. For instance, moderate acid
484 fracturing may be used to dissolve calcite films, and CO₂ dissolved in water can also
485 partially dissolve calcite layers on early fracture surfaces.

486 **4.4 A New Perspective on Fracture Numerical Simulation**

487 When the mechanical model is updated and the mechanism of fracture generation and
488 evolution is redefined, numerical modeling software and algorithms must also be adjusted
489 accordingly. First and foremost, the origin of fracture space must be incorporated, followed
490 by modeling the initiation and propagation of fractures, and ultimately the transport range of
491 proppants.

492 As of the writing of this paper, a review of representative literature reveals that
493 understanding of the stress field associated with hydraulic fracturing still largely relies on the
494 mechanical framework proposed by Hubbert and Willis (1957)[7]. This includes the
495 assumption that the main fracture is tensile in nature and that the medium is a homogeneous
496 elastic body. There remains a lack of detailed studies describing the progressive
497 development of fractures, leading to fundamental flaws in current numerical simulation
498 approaches for fracture modeling.

499 **4.5 Deficiencies in Fracture Toughness Testing Methods**

500 In Chapter 3 (page 3-20) of the third edition of *Reservoir Stimulation*[4] the
501 experimental method for determining fracture toughness involves applying tensile force.
502 However, this approach does not reflect actual subsurface conditions, and the fracture
503 toughness values obtained are likely underestimated. As a result, the fracture initiation
504 pressures used in fracturing design are too low, which directly compromises fracturing
505 performance.

506 Under the confined-space model, high-pressure fluid should be injected through a
507 central borehole, and the sample should be held under constraint. Such a testing environment

508 would more accurately simulate the realistic in-situ stress conditions encountered
509 underground

510

511 **5. Understanding and Significance**

512 **5.1 New Insights**

513 **5.1.1 The Influence of Confined Space on the Fracturing Process**

514 Under the constraint of a confined space, the stress state of the rock during fracturing
515 undergoes significant changes. Fracture width is mainly determined by the degree of
516 compressive deformation, while differential deformation induces shear. Fracture tip
517 propagation depends on tensile forces generated by the overall displacement of the rock
518 mass. This fundamentally differs from the "volume expansion" concept in traditional
519 open-space models and emphasizes the limiting role of surrounding rock on fracture
520 growth—representing a compressive stress field rather than a tensile one.

521 **5.1.2 A New Perspective on Production Enhancement Mechanism**

522 The primary contributor to enhanced production in large-volume hydraulic fracturing is
523 not solely the conductivity of newly created fractures. More critically, it is the significant
524 increase in reservoir fluid pressure after fracturing. As fracturing fluid enters the formation,
525 the existing pore space is compressed, raising the fluid pressure and thereby increasing the
526 driving force for hydrocarbon flow. New and pre-existing fractures serve mainly as channels
527 for pressure transmission and redistribution, rather than just as fluid pathways.

528 **5.1.3 New Parameters for Evaluating Fracturing Effectiveness**

529 Traditional evaluations of fracturing success are based mainly on fracture geometry, but
530 this method fails to fully capture the production enhancement effects under the
531 confined-space model. Based on the new understanding, parameters such as residual
532 proppant volume and post-fracturing reservoir fluid pressure should be introduced to more
533 accurately assess the effectiveness of reservoir stimulation.

534 **5.1.4 Rethinking the Production Mechanism**

535 There are misconceptions in understanding the mechanism of production enhancement
536 after fracturing—placing too much emphasis on fracture geometry while ignoring the crucial
537 role of increased pore pressure. This misalignment has skewed the objectives of fracturing
538 operations. A shift in perspective is needed—from generating local fractures to modifying
539 the reservoir as a whole.

540 **5.2 Geological Significance**

541 **5.2.1 Well Placement and Trajectory Optimization**

542 In heterogeneous reservoirs such as shale oil and tight oil formations, differential
543 compressive deformation is pronounced, and the internal stress distribution is
544 uneven—making shear fracture formation more likely. Therefore, well placement and
545 trajectory design should prioritize high-heterogeneity zones and formations with significant
546 compressive variation to maximize activation of the reservoir's potential flow space.

547 **5.2.2 Enhancing Reservoir Utilization and Recovery Factor**

548 By strengthening differential deformation, not only can a more effective fracture
549 network be developed, but the overall utilization of the reservoir can also be significantly
550 improved. This holistic stimulation strategy is particularly effective in low-permeability
551 reservoirs, where it can notably increase the oil recovery factor and ultimate recovery.

552 **5.3 Engineering Significance**

553 **5.3.1 Optimizing Fracturing Design**

554 Through refined design, the degree of differential deformation in the rock mass during
555 fracturing can be increased, leading to the creation of more complex fracture networks.
556 Meanwhile, optimizing the staging and sequence of proppant injection enhances overall
557 proppant placement efficiency.

558 **5.3.2 Well Trajectory Optimization**

559 While ensuring casing integrity, the horizontal section of the well should be as parallel
560 as possible to the direction of minimum principal stress. This facilitates the formation of
561 slice-like fracture structures, which not only reduce wellbore interference but also make full
562 use of the natural stress field to achieve more uniform and farther-reaching fractures.

563 **5.3.3 Proppant Optimization**

564 By reducing fluid volume and increasing proppant concentration, proppants of varied
565 sizes can be injected sequentially into the formation, enhancing differential deformation,
566 generating more shear fractures, and further increasing reservoir fluid pressure. During the
567 flowback stage, minimizing proppant return not only maintains fracture conductivity but also
568 helps retain the elevated post-fracturing reservoir pressure, providing sustained driving
569 energy for hydrocarbon production.

570

571 **6. Conclusions**

572 1. Artificial fractures and proppant-bearing spaces formed under a confined space
573 system are the result of adjustment and redistribution of pre-existing pore space. Differential
574 compaction-induced deformation is the mechanical basis for the formation of shear fractures.
575 The sequential process of rock deformation and failure is: compression (creating fracture

576 space) → tension (controlling fracture propagation direction) → differential deformation
577 (generating shear fractures).

578 2. Reservoir fluid pressure increase is a key controlling factor for production
579 enhancement through hydraulic fracturing. Based on this mechanism, well placement and
580 trajectory design can be further optimized, target intervals for fracturing can be better
581 selected, and reservoir utilization and recovery efficiency can be improved. This also
582 provides a new conceptual framework for numerical simulation of reservoir development.

583 3. Post-reservoir formation processes such as compaction of the strata, secondary growth
584 of diagenetic minerals, and the swelling of clay minerals can all increase the fluid pressure
585 within the reservoir, which is conducive to enhancing the recovery factor of oil and gas field
586 development.

587 4. The effectiveness of hydraulic fracturing can be quantitatively evaluated and
588 production can be predicted using the three-dimensional distribution of porosity and the
589 post-fracturing reservoir fluid pressure parameters, which yields better results than relying
590 on fracture geometry obtained through microseismic monitoring.

591

592 **Acknowledgements**

593 The author would like to express sincere gratitude to Senior Engineers Yang Yihua and Xie Jilong, as
594 well as Professor Zeng Zuoxun, for their valuable guidance during the conception and writing of this
595 paper.

596

597 **REFERENCE**

- 598 1. Belyadi, H., Fathi, E., & Belyadi, F. (2019). *Hydraulic Fracturing in Unconventional Reservoirs: Theories, Operations, and Economic Analysis*. Gulf Professional Publishing.
- 599 2. Berkowitz, B. (2002). Characterizing Flow and Transport in Fractured Geological Media: A Review. *Advances in Water Resources*, 25(8-12), 861-884.
- 600 3. Biot, M. A. (1941). General Theory of Three-Dimensional Consolidation. *Journal of Applied Physics*, 12(2), 155-164.
- 601 4. Economides, M. J., & Nolte, K. G. (2000). *Reservoir Stimulation* (3rd ed.). Wiley.
- 602 5. Fisher, M. K., & Warpinski, N. R. (2012). Hydraulic-Fracture-Height Growth: Real Data. *SPE Production & Operations*, 27(1), 8-19.
- 603 6. Geertsma, J., & de Klerk, F. (1969). A Rapid Method of Predicting Width and Extent of Hydraulically Induced Fractures. *Journal of Petroleum Technology*, 21(12), 1571-1581
- 604 7. Hubbert, M. K., & Willis, D. G. (1957). Mechanics of Hydraulic Fracturing. *Transactions of the AIME*, 210, 153-168.
- 605
- 606
- 607
- 608
- 609
- 610

- 611 8. Maghsoudi, S., & Eaton, D. W. (2016). Nontrivial clustering of microseismicity induced by hydraulic
612 fracturing. *Geophysical Research Letters*, 43(19), 10310–10317.
613 <https://doi.org/10.1002/2016GL070983>
- 614 9. Mayerhofer, M. J., Lonon, E. P., Warpinski, N. R., et al. (2010). What is Stimulated Reservoir Volume
615 (SRV)? *SPE Production & Operations*, 25(1), 89-98.
- 616 10. Miehe, C., Hofacker, M., & Welschinger, F. (2010). A Phase Field Model for Rate-Independent Crack
617 Propagation: Robust Algorithmic Implementation Based on Operator Splits. *Computer Methods in
618 Applied Mechanics and Engineering*, 199(45-48), 2765-2778.
- 619 11. Miskimins, J. L. (Ed.). (2019). *Hydraulic Fracturing: Fundamentals and Advancements*. Society of
620 Petroleum Engineers.
- 621 12. Olson, J. E., & Dahi-Taleghani, A. (2010). Modeling Simultaneous Growth of Multiple Hydraulic
622 Fractures and Their Interaction with Natural Fractures. In *SPE Hydraulic Fracturing Technology
623 Conference*, SPE-119739-MS.
- 624 13. Perkins, T. K., & Kern, L. R. (1961). Widths of Hydraulic Fractures. *Journal of Petroleum Technology*,
625 13(9), 937-949.
- 626 14. Vavryčuk, V. (2008). Non-double-couple mechanisms of microearthquakes induced
627 during the 2000 injection experiment at the KTB site, Germany: A result of tensile
628 faulting or anisotropy of a rock? *Tectonophysics*, 456(1-2), 74-93.
629 <https://doi.org/10.1016/j.tecto.2008.05.026>
- 630 15. Wang, C., Liang, C., Deng, K., Huang, Y., & Zhou, L. (2018). Spatiotemporal Distribution of
631 Microearthquakes and Implications Around the Seismic Gap Between the Wenchuan and Lushan
632 Earthquakes. *Tectonics*, 37(8), 2695–2709. <https://doi.org/10.1029/2018TC005000>
- 633 16. Warpinski, N. R., Mayerhofer, M. J., Vincent, M. C., et al. (2009). Stimulating Unconventional
634 Reservoirs: Maximizing Network Growth While Optimizing Fracture Conductivity. In *SPE
635 Unconventional Reservoirs Conference*, SPE-114173-MS.
- 636 17. Zhang, H., Eaton, D. W., Li, G., Liu, Y., & Harrington, R. M. (2022). Spatiotemporal Variations in
637 Earthquake Triggering Mechanisms During Multistage Hydraulic Fracturing in Western Canada.
638 *Journal of Geophysical Research: Solid Earth*, 127(9), e2022JB024744.
639 <https://doi.org/10.1029/2022JB024744>
- 640 18. Zoback, M. D. (2010). *Reservoir Geomechanics*. Cambridge University Press.
- 641 19. Zoback, M. D., & Kohli, A. H. (2019). *Unconventional Reservoir Geomechanics: Shale Gas, Tight Oil,
642 and Induced Seismicity*